

Room for an $S = +1$ pentaquark in K^+ - nucleus phenomenology

A. Gal¹ and E. Friedman¹

¹*Racah Institute of Physics, The Hebrew University, Jerusalem 91904, Israel*

Evidence for excitation of exotic $S = +1$ pentaquark degrees of freedom is presented by studying optical-potential fits to K^+ - nucleus total, reaction and elastic-differential cross section data at $p_{\text{lab}} \sim 500 - 700$ MeV/c. Estimates of the underlying two-nucleon absorption $K^+ nN \rightarrow \Theta^+ N$ reaction cross section are made and are used for discussing the anticipated cross section of the strangeness exchange reaction $K^+ N \rightarrow \pi \Theta^+$.

PACS numbers: 13.75.Jz, 14.80.-j, 25.80.Nv

I. INTRODUCTION

Conclusive direct evidence for the existence of an exotic $S=1$, $I=0$, $Z=1$ pentaquark baryon, the $\Theta^+(1540)$ [1], is still lacking. Dedicated experiments using photons, pions and kaons are expected to collect in due course sufficiently high statistics in order to resolve this issue. However, in Ref. [2] we have noted that the $\Theta^+(1540)$ provides a new mode of reactivity to K^+ - nuclear interactions with possibly large effects on K^+ - nuclear total and reaction cross sections in the energy range above its threshold in nuclei, $p_{\text{lab}}^{\text{th}} \sim 400$ MeV/c. Since the $K^+ N$ interaction in this energy range appears to be fairly weak and featureless, without visible evidence for $KN \rightarrow \Theta^+$ coupling to exotic $qqqq\bar{s}$ configurations, pentaquark degrees of freedom in *nuclei* could be more readily excited on two-nucleon clusters: $KNN \rightarrow \Theta^+ N$. This is related to the virtual two-meson decay mode $\Theta^+ \rightarrow NK\pi$ [3, 4]. In our earlier work we demonstrated how pentaquark production, corresponding to the underlying two-nucleon absorption mode

$$K^+ nN \rightarrow \Theta^+ N, \quad (1)$$

could contribute to the total and reaction cross sections [5, 6] extracted from transmission experiments [7, 8] at the Brookhaven National Laboratory (BNL) Alternating Gradient Synchrotron (AGS) on ${}^6\text{Li}$, ${}^{12}\text{C}$, ${}^{28}\text{Si}$ and ${}^{40}\text{Ca}$ at four energies, for $p_{\text{lab}} = 488, 531, 656, 714$ MeV/c. Our considerations are based merely on the observation [5, 6] that these K^+ - nucleus cross sections exhibit excessive reactivity, some 10 – 20% over the reactivity provided by the KN interaction, even after allowance is made for conventional nuclear medium effects. The suggestion that $S = +1$ pentaquark degrees of freedom give rise to this excess reactivity does not require that the Θ^+ pentaquark has particular spin-parity values nor that it is as narrow as argued (less than $\Gamma \sim 1$ MeV) by analyzing K^+ initiated production processes [9, 10, 11].

In the present work we provide a more detailed account of the calculations presented briefly in Ref. [2] for total and reaction cross sections, extending these calculations to include also K^+ elastic scattering data at $p_{\text{lab}} = 715$ MeV/c on ${}^6\text{Li}$ and ${}^{12}\text{C}$ [12, 13]. Having determined the strength of the K^+ absorption mode Eq. (1), we then

discuss its relationship to the cross section level expected for the $K^+ p \rightarrow \pi^+ \Theta^+$ production reaction which is under active experimentation in KEK at present [14].

II. METHODOLOGY

The starting form adopted in our calculations for the kaon-nucleus optical potential V_{opt} is the simplest possible $t\rho$ form:

$$2\varepsilon_{\text{red}}^{(A)} V_{\text{opt}}(r) = -4\pi F_A b_0 \rho(r), \quad (2)$$

where $\varepsilon_{\text{red}}^{(A)}$ is the center-of-mass (c.m.) reduced energy,

$$(\varepsilon_{\text{red}}^{(A)})^{-1} = E_p^{-1} + E_A^{-1} \quad (3)$$

in terms of the c.m. total energies for the projectile and target respectively, and

$$F_A = \frac{M_A \sqrt{s}}{M(E_A + E_p)} \quad (4)$$

is a kinematical factor resulting from the transformation of amplitudes between the KN and the K^+ - nucleus c.m. systems, with M the free nucleon mass, M_A the mass of the target nucleus and \sqrt{s} the total projectile-nucleon energy in their c.m. system. The parameter b_0 in Eq. (2) reduces in the impulse approximation to the (complex) isospin-averaged KN scattering amplitude in the forward direction. The optical potential V_{opt} is inserted into the Klein Gordon equation, of the form used in our previous calculations:

$$\left[\nabla^2 + k^2 - (2\varepsilon_{\text{red}}^{(A)}(V_c + V_{\text{opt}}) - V_c^2) \right] \psi = 0 \quad (5)$$

in units of $\hbar = c = 1$. Here k is the wave number in the c.m. system, and V_c is the Coulomb potential due to the charge distribution of the nucleus. These forms of the potential and the equation take into account $1/A$ corrections, which is an important issue when handling as light a nucleus as ${}^6\text{Li}$.

The nuclear density $\rho(r)$ is an essential ingredient of the optical potential V_{opt} in Eq. (2). The density distribution of the protons is usually considered known as it

TABLE I: values of $\bar{\rho}$ (in fm^{-3}) Eq. (6), for the two sets of point-nucleon densities defined at the end of Sec. II.

density	${}^6\text{Li}$	${}^{12}\text{C}$	${}^{28}\text{Si}$	${}^{40}\text{Ca}$
(i)	0.049	0.104	0.112	0.112
(ii)	0.049	0.104	0.105	0.107

is obtained from the nuclear charge distribution [15] by unfolding the proton charge distribution. For ${}^6\text{Li}$ and for ${}^{12}\text{C}$ the modified harmonic oscillator (MHO) form was used whereas for ${}^{28}\text{Si}$ and for ${}^{40}\text{Ca}$ the two-parameter Fermi (2pF) form was used. In all cases the parameters were obtained numerically, requiring that folding in the finite-size proton charge distribution will generate a good fit to the nuclear charge distribution. For these $N = Z$ nuclei we assumed in our previous analysis [2] that the neutron densities are identical to the corresponding proton densities. This choice is marked (i) in Table I. In the present work we have adopted also a slightly different approach for the two heavier targets. Using the 2pF densities we obtained the parameters for the proton distributions by approximate analytical unfolding of the charge distribution [16]. The neutron densities were assumed to have an ‘average’ shape [17, 18] with a root-mean-square (rms) radius r_n given by $r_n - r_p = -0.0162A^{1/3}$ fm (only for $N = Z$ nuclei). This choice is marked (ii) in Table I. By using two slightly different sets of densities we could test sensitivities of the derived potential parameters.

III. RESULTS

A. K^+ - nucleus total and reaction cross sections

As reviewed recently in the Introduction of Ref. [2], the simple $t\rho$ form of V_{opt} in Eq. (2) does not provide a satisfactory fit to the K^+ - nuclear integral cross section data at several hundreds of MeV. Indeed, using the methodology outlined above, it was shown by Friedman *et al.* [5] that no *effective* value for b_0 could be found that fits satisfactorily the reaction and total cross sections derived from the BNL-AGS transmission measurements at $p_{\text{lab}} = 488, 531, 656, 714$ MeV/c on ${}^6\text{Li}$, ${}^{12}\text{C}$, ${}^{28}\text{Si}$, ${}^{40}\text{Ca}$. This is demonstrated in the upper part of Fig. 1 for the reaction cross sections per nucleon σ_R/A at 488 MeV/c, where the calculated cross sections using a best-fit $t\rho$ optical potential (dashed line) are compared with the experimental values listed in Ref. [6]. The best-fit values of $\text{Re } b_0$ and $\text{Im } b_0$ which specify this $t\rho$ potential are given in the first row of Table II, where $\text{Im } b_0$ represents 10 – 15% increase with respect to the free-space value given in the line underneath. The χ^2/N of this density-independent fit is very high. Its failure is due to the impossibility to reconcile the ${}^6\text{Li}$ data (which for the total cross sections are consistent with the K^+d ‘elementary’ cross sections) with the data on the other, denser nuclei, as is clearly exhibited in Fig. 1 for the best-fit $t\rho$

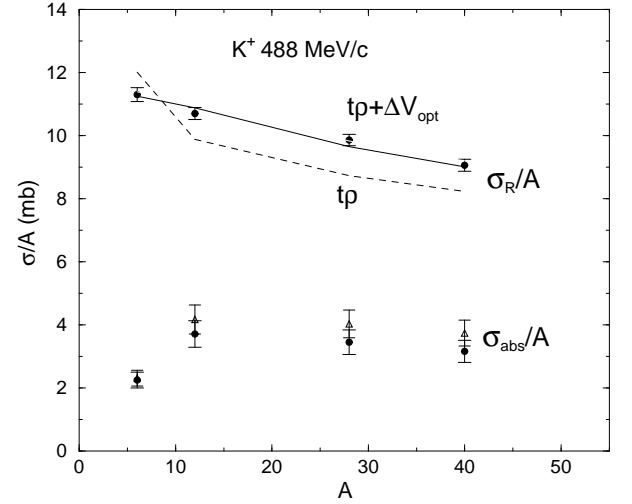


FIG. 1: Data and calculations [2] for K^+ reaction cross sections per nucleon (σ_R/A) at $p_{\text{lab}} = 488$ MeV/c are shown in the upper part. Calculated K^+ absorption cross sections per nucleon (σ_{abs}/A) are shown in the lower part, see text.

TABLE II: Fits to K^+ - nuclear integral cross sections [5, 6] at $p_{\text{lab}} = 488$ MeV/c, using Eqs. (5) - (7).

V_{opt}	$\text{Re } b_0$ (fm)	$\text{Im } b_0$ (fm)	β (fm^3)	ρ_{th} (fm^{-3})	χ^2/N
$t\rho$	-0.205(27)	0.173(7)	—	—	18.2
$t_{\text{free}}\rho$	-0.178	0.153			
Eq. (7)	-0.154(12)	0.160(2)	12.4(38)	0.088(6)	0.06

dashed line. If ${}^6\text{Li}$ is removed from the data base, then it becomes possible to fit reasonably well the data for the rest of the nuclei, but the rise in $\text{Im } b_0$ with respect to its free-space value is then substantially higher than that for the $t\rho$ fits which exclude ${}^6\text{Li}$ is included. At the higher energies, $t\rho$ fits which exclude ${}^6\text{Li}$ are less successful than at 488 MeV/c, while also requiring a substantial rise in $\text{Im } b_0$, which means increased values of the in-medium KN total cross sections with respect to the corresponding free-space values. This has been observed also in a K^+ - nucleus quasifree-scattering analysis [19], for K^+ mesons incident on C, Ca, Pb at $p_{\text{lab}} = 705$ MeV/c [20].

An effective way of discriminating between ${}^6\text{Li}$ and the denser nuclei was established *empirically* in Refs. [5, 6] by requiring that the imaginary (absorptive) part of the K^+ - nucleus optical potential gets significantly enhanced whenever the average nuclear density

$$\bar{\rho} = \frac{1}{A} \int \rho^2 d\mathbf{r} \quad (6)$$

exceeds a threshold nuclear density ρ_{th} . Specifically, if $\text{Im } V_{\text{opt}}$ in Eq. (2) is modified as follows,

$$\text{Im } b_0 \rho(r) \rightarrow \text{Im } b_0 \rho(r) [1 + \beta (\bar{\rho} - \rho_{\text{th}}) \Theta(\bar{\rho} - \rho_{\text{th}})], \quad (7)$$

then the long-standing problem of the reaction and total cross sections derived from the BNL-AGS transmission

measurements at $p_{\text{lab}} = 488, 531, 656, 714$ MeV/c on ${}^6\text{Li}$, ${}^{12}\text{C}$, ${}^{28}\text{Si}$, ${}^{40}\text{Ca}$ is resolved. This is demonstrated in Table II, showing two fits to the $N = 8$ data points at 488 MeV/c, which is the closest momentum to the Θ^+ resonance. The first fit in the table, as explained above, uses only density-independent fitted values for the complex parameter b_0 in Eq. (2). The second fit in the table introduces density dependence through Eq. (7) and the resulting improvement as judged by the value of χ^2/N is spectacular. When considering all 32 data points available at the 4 energies [6], using the same values for β and ρ_{th} independently of energy, then the $\chi^2/N = 42.7$ for the best-fit $t\rho$ potential is reduced to 0.65 using this empirical modification Eq. (7). The well-determined value of ρ_{th} is considerably higher than the average nuclear density $\bar{\rho}$ for ${}^6\text{Li}$ (about 0.05 fm^{-3}), but is lower than the $\bar{\rho}$ values appropriate to the other, denser targets (about 0.1 fm^{-3}) as shown in Table I. This spectacular fit clearly suggests that new absorptive degrees of freedom open up above the threshold nuclear density of 0.09 fm^{-3} . We have argued in Ref. [2] that the Θ^+ may provide for such a new degree of freedom via K^+ absorption on two nucleons, $K^+nN \rightarrow \Theta^+N$, with threshold at $p_{\text{lab}}^{\text{th}} \sim 400$ MeV/c.

Here we have incorporated $K^+nN \rightarrow \Theta^+N$ two-nucleon absorption into the impulse-approximation motivated $V_{\text{opt}}(r)$, Eq. (2), by adding a $\rho^2(r)$ piece, as successfully practised in pionic atoms [21, 22] to account for π^- absorption on two nucleons:

$$b_0 \rho(r) \rightarrow b_0 \rho(r) + B \rho^2(r), \quad (8)$$

where the parameter B represents the effect of K^+ nuclear absorption into exotic $S = +1$ baryonic channels. Using this potential we have repeated fits to all 32 data points for the reaction and total cross sections. This resulted in a substantial improvement of the quality of the fit, compared to the $t\rho$ potential. However, the fits at the higher momenta are not as successful as the fit at 488 MeV/c, suggesting that one needs a more effective way to distinguish between ${}^6\text{Li}$ and the denser nuclear targets. In fact, as demonstrated in Table II above, the average nuclear density $\bar{\rho}$, Eq. (6), provides for such discrimination and is instrumental in achieving good agreement with experiment. We therefore replace Eq. (8) by the simplest ansatz

$$b_0 \rho(r) \rightarrow b_0 \rho(r) + B \bar{\rho} \rho(r). \quad (9)$$

The added piece is a functional of the density which to lowest order reduces to a ρ^2 form. Below we compare the two extensions of V_{opt} offered by Eqs. (8) and (9) and comment on the significance of the results obtained using the less founded form Eq. (9).

Fits to the total and reaction cross section data [6], using Eqs. (8) and (9) with our set of slightly revised densities described above, are exhibited in Table III. It is clear that the quality of fit improves dramatically with respect to the (also shown) $t\rho$ best fits upon allowing for K^+ absorption (parameter B). The superiority of the $\bar{\rho}\rho$

TABLE III: Fits to the eight K^+ - nuclear integral cross sections [6] at each of the four laboratory momenta p_{lab} (in MeV/c), using different potentials.

p_{lab}	V_{opt}	$\text{Re}b_0(\text{fm})$	$\text{Im}b_0(\text{fm})$	$\text{Re}B(\text{fm}^4)$	$\text{Im}B(\text{fm}^4)$	χ^2/N
488	$t\rho$	-0.203(26)	0.172(7)			16.3
	$t_{\text{free}}\rho$	-0.178	0.153			
	Eq.(8)	-0.178	0.122(5)	0.52(20)	0.88(8)	1.18
	Eq.(9)	-0.178	0.129(4)	0.17(11)	0.62(6)	0.27
531	$t\rho$	-0.196(39)	0.202(9)			56.3
	$t_{\text{free}}\rho$	-0.172	0.170			
	Eq.(8)	-0.172	0.155(14)	1.79(46)	0.72(27)	7.01
	Eq.(9)	-0.172	0.146(5)	0.46(21)	0.78(7)	3.94
656	$t\rho$	-0.220(50)	0.262(12)			54.9
	$t_{\text{free}}\rho$	-0.165	0.213			
	Eq.(8)	-0.165	0.203(18)	1.66(80)	0.89(36)	7.24
	Eq.(9)	-0.165	0.204(5)	2.07(19)	0.77(7)	0.32
714	$t\rho$	-0.242(53)	0.285(15)			67.7
	$t_{\text{free}}\rho$	-0.161	0.228			
	Eq.(8)	-0.161	0.218(24)	1.40(95)	1.10(48)	9.3
	Eq.(9)	-0.161	0.218(6)	1.51(43)	0.97(9)	1.24

version (marked as ‘Eq. (9)’) compared to the ρ^2 version (marked as ‘Eq. (8)’) is also very clearly observed. The calculated reaction cross sections at 488 MeV/c, using Eq. (9), are shown by the solid line marked $t\rho + \Delta V_{\text{opt}}$ in the upper part of Fig. 1, where ΔV_{opt} is the added piece of V_{opt} due to a nonzero value of B . Clearly, it is a very good fit. Very recently, Tolos *et al.* [4] have demonstrated that a similarly substantial improvement in the reproduction of reaction cross sections could be achieved microscopically by coupling in degrees of freedom of the $\Theta^+(1540)$ pentaquark.

We note that the splitting of $\text{Im } V_{\text{opt}}$ in Table III into its two reactive components $\text{Im } b_0$ and $\text{Im } B$ appears well determined by the data at all energies, and perhaps is even model independent, particularly for the $\bar{\rho}\rho$ version Eq. (9) of the optical potential for which very accurate values of $\text{Im } b_0$ are derived. These values of $\text{Im } b_0$ are close to, but somewhat below the corresponding free-space values, in agreement with the conventional $t\rho \rightarrow g\rho$ medium effects considered in Ref. [4]. This is not the case for $\text{Re } V_{\text{opt}}$ where its two components are correlated strongly when $\text{Re } b_0$ is varied too, largely cancelling each other into a resultant poorly determined $\text{Re } V_{\text{opt}}$. Therefore, in Table III we show results only for $\text{Re } b_0$ held fixed at its free-space value.

Table III suggests that the two-nucleon absorption coefficient $\text{Im } B$ rises slowly with energy as appropriate to the increased phase space available to the underlying two-nucleon absorption process $K^+nN \rightarrow \Theta^+N$. Its values in this energy range are roughly independent of the form of ΔV_{opt} , the more conservative Eq. (8) or the more effective Eq. (9), used to derive these values from the data. This stability of the results for $\text{Im } B$ is of special importance for the interpretation offered here.

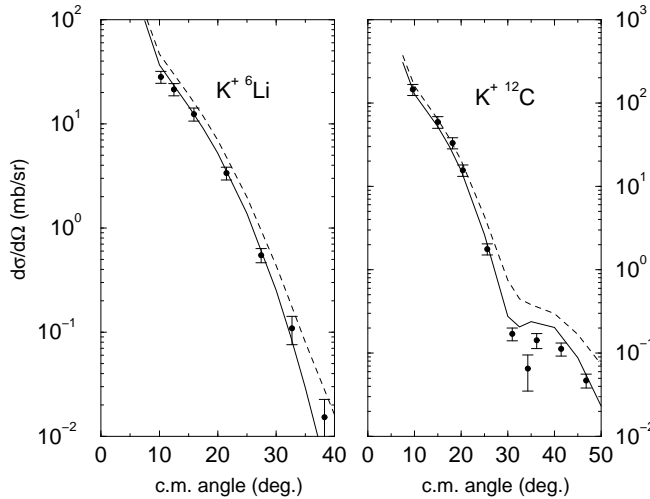


FIG. 2: Comparison between measured differential cross sections for K^+ elastic scattering at $p_{\text{lab}} = 715$ MeV/c on ${}^6\text{Li}$ and ${}^{12}\text{C}$ [13] and best-fit calculations using Eq. (8) (dashed lines) and Eq. (9) (solid lines).

Regarding $\text{Re } V_{\text{opt}}$, and recalling that $\bar{\rho} \sim 0.1 \text{ fm}^{-3}$ for the dense nuclear targets, it is clear that $\text{Re } V_{\text{opt}} \sim 0$ at the two higher momenta, illustrating the inadequacy of the $t\rho$ model which does not produce this trend. We note that our $K^+nN \rightarrow \Theta^+N$ absorption reaction is related to the mechanism proposed recently in Ref. [3] as causing strong Θ^+ - nuclear attraction, based on $K\pi$ two-meson cloud contributions to the self energy of Θ^+ in nuclear matter. However, it would appear difficult to reconcile as strong Θ^+ - nuclear attraction as proposed there with the magnitude of $\text{Re } B$ derived in the present work.

B. K^+ elastic scattering differential cross sections

In order to further test the picture that emerges from the analysis of the integral cross sections for the K^+ - nucleus interaction, we repeated the analysis including also differential cross sections for the elastic scattering of K^+ by some of the target nuclei. Such data exist for scattering of 715 MeV/c K^+ by ${}^6\text{Li}$ and by ${}^{12}\text{C}$ [12, 13]. Similar data at 635 MeV/c were not included because integral cross sections are not available at that energy. Experience had shown that in situations where the real part of the optical potential has a repulsive part, or at least is not predominantly attractive, then fits to only angular distributions may lead to values of potential parameters that result in most unacceptable calculated values for reaction and total cross sections. In other words, under such circumstances the integral cross sections serve as powerful constraints on the potential parameters derived from fitting to differential cross sections [23].

Fits were made to the combined integral and differential cross sections at 714 MeV/c consisting of the eight integral cross sections and the 17 differential cross sections

from Ref. [13], using the potentials of either Eq. (8) or Eq. (9). For the latter potential and for the combined 25 data points we obtained $\chi^2/N = 5.3$, with $\chi^2/N = 1.4$ for the integral cross sections and $\chi^2/N = 6.8$ for the differential cross sections. Using Eq. (8) instead, we get a considerably inferior fit with $\chi^2/N = 24.6$. Potential parameters for Eq. (9) are $\text{Re } b_0 = -0.161$ fm (fixed), $\text{Im } b_0 = 0.219 \pm 0.011$ fm, $\text{Re } B = 1.57 \pm 0.56$ fm and $\text{Im } B = 0.94 \pm 0.15$ fm. These results are in perfect agreement with the corresponding values in Table III, obtained from fits to integral cross sections only. Figure 2 shows comparisons between calculations and experiment for the elastic scattering from ${}^6\text{Li}$ and ${}^{12}\text{C}$ for the best-fit potentials for both Eq. (8) (dashed) and Eq. (9) (solid curves). The superiority of the $\bar{\rho}\rho$ form is clear. Using the 14 differential cross section data of Ref. [12] instead of the 17 data points of Ref. [13], together with the integral cross sections, leads to slightly lower values of χ^2 but the potential parameters are virtually the same as for the fits using the data of Ref. [13].

C. K^+ absorption cross sections

By analogy to analyses of pionic atoms [21, 22] and low-energy pion-nuclear scattering reactions [23, 24], the additional piece ΔV_{opt} due to the nonzero value of the absorption parameter B is responsible for K^+ nuclear absorption into Θ^+ - nuclear final states. One way to estimate the absorption cross section $\sigma_{\text{abs}}^{(K^+)}$ is to use the distorted-wave Born approximation:

$$\sigma_{\text{abs}}^{(K^+)} \sim -\frac{2}{\hbar v} \int \text{Im}(\Delta V_{\text{opt}}(r)) |\Psi_{(\Delta V_{\text{opt}}=0)}^{(+)}(\mathbf{r})|^2 d\mathbf{r} \quad (10)$$

where the distorted waves $\Psi_{(\Delta V_{\text{opt}}=0)}^{(+)}$ are calculated discarding ΔV_{opt} . Recall that for $B = 0$, replacing in the above integral $\Delta V_{\text{opt}}(r)$ by $V_{\text{opt}}(r)$ gives the total reaction cross section in the absence of the $K^+nN \rightarrow \Theta^+N$ channel. However, the precise expression for the total reaction cross section in the presence of this absorption mode into Θ^+ - nucleus final states requires the use of the fully distorted waves $\Psi^{(+)}$, so that a different approximation for the absorption cross section is given by

$$\sigma_{\text{abs}}^{(K^+)} \sim -\frac{2}{\hbar v} \int \text{Im}(\Delta V_{\text{opt}}(r)) |\Psi^{(+)}(\mathbf{r})|^2 d\mathbf{r} \quad (11)$$

Calculated absorption cross sections *per target nucleon* at $p_{\text{lab}} = 488$ MeV/c are shown in the lower part of Fig. 1 for the fit using Eq. (9) for V_{opt} in Table III. The triangles are for expression (10) and the solid circles are for expression (11). The error bars plotted are due to the uncertainty in the parameter $\text{Im } B$. It is seen that these calculated absorption cross sections, for the relatively dense targets of C, Si and Ca, are proportional to the mass number A , and the cross section per target nucleon due to $\text{Im } B \neq 0$ is estimated as close to

3.5 mb. Although the less successful Eq. (8) gives cross sections larger by 40% at this particular incident momentum, this value should be regarded an upper limit, since the best-fit density-dependent potentials of Refs. [5, 6] yield values smaller than 3.5 mb by a similar amount. The experience gained from studying π -nuclear absorption [24] leads to the conclusion that $\sigma_{\text{abs}}(K^+NN)$ is smaller than the extrapolation of $\sigma_{\text{abs}}^{(K^+)}/A$ in Fig. 1 to $A = 1$, and since the KN interaction is weaker than the πN interaction one expects a reduction of roughly 50%, so that $\sigma_{\text{abs}}(K^+NN) \sim 1 - 2$ mb.

We note in Fig. 1 the considerably smaller absorption cross section per nucleon calculated for ${}^6\text{Li}$ which, considering its low density, suggests a cross section of order fraction of millibarn for $K^+d \rightarrow \Theta^+p$, well below the order 1 mb which as Gibbs has argued recently [10] could indicate traces of Θ^+ in K^+d total cross sections near $p_{\text{lab}} \sim 440$ MeV/c. To be definite, we suggested in Ref. [2] the following range of values for this cross section:

$$\sigma(K^+d \rightarrow \Theta^+p) \sim 0.1 - 0.5 \text{ mb} . \quad (12)$$

This provides a quantitative estimate for a possible missing-mass search for $\Theta^+(1540)$ by observing the final proton, while the signal cross section need not exhibit a resonance behavior as function of the incoming K^+ momentum.

IV. DISCUSSION

We have provided a cross-section estimate, Eq. (12), for the *two-nucleon* production reaction $K^+d \rightarrow \Theta^+p$. It is worth emphasizing that this cross section is considerably larger than what a *one-nucleon* production process $KN \rightarrow \Theta^+$ would induce on a deuteron target. Examples of one-step production processes in which the Θ^+ is produced on one of the nucleons in a quasi on-shell kinematics are:

$$K^+ p \rightarrow K^+ p , \quad K^+ n \rightarrow \Theta^+ , \quad (13)$$

$$K^+ n \rightarrow K^0 p , \quad K^0 p \rightarrow \Theta^+ , \quad (14)$$

in which the Θ^+ production is accompanied by initial scattering, or

$$K^+ n \rightarrow \Theta^+ , \quad \Theta^+ p \rightarrow \Theta^+ p , \quad (15)$$

in which it is followed by final scattering on the other ‘spectator’ nucleon. The last process Eq. (15) may be compared to a similar pion absorption process near the (3,3) resonance energy where the Δ is produced approximately on-shell, subsequently rescattering on the other nucleon, for example:

$$\pi^+ p \rightarrow \Delta^{++} , \quad \Delta^{++} n \rightarrow p p , \quad (16)$$

with a sizable cross section [24]

$$\sigma(\pi^+d \rightarrow pp) \sim 12.5 \text{ mb} . \quad (17)$$

Scaling by the ratio of coupling constants squared $g_{KN\Theta}^2/g_{\pi N\Delta}^2 \sim 2.5 \times 10^{-3}$, assuming $J^\pi(\Theta^+) = (\frac{1}{2})^+$ and $\Gamma(\Theta^+ \rightarrow KN) \sim 1$ MeV, we estimate a cross section level of 0.03 mb for the one-step production process at the Θ^+ resonance energy. [Assuming $J^\pi(\Theta^+) = (\frac{1}{2})^-$, the one-step production cross section is lower by at least another order of magnitude.] The one-step cross section affordable by the neutron Fermi motion at $p_{\text{lab}} = 488$ MeV/c would be considerably smaller than this estimate which holds at the very vicinity of the Θ^+ mass for $p_{\text{lab}} = 440$ MeV/c. In contrast, the two-nucleon reaction need not involve the suppressed $KN\Theta$ coupling and its cross section which we have estimated in Eq. (12) for $p_{\text{lab}} = 488$ MeV/c should vary slowly with the kaon energy. The simplest mechanism for a two-nucleon K^+ absorption process could be envisaged by letting an intermediate off-shell pion correlate two target nucleons, viz.

$$K^+ p \rightarrow \pi^+ \Theta^+ , \quad \pi^+ n \rightarrow p , \quad (18)$$

or

$$K^+ n \rightarrow \pi^0 \Theta^+ , \quad \pi^0 p \rightarrow p , \quad (19)$$

where the threshold for the $K^+N \rightarrow \pi\Theta^+$ reaction occurs at $p_{\text{lab}} \sim 760$ MeV/c in free space, and getting as low as $p_{\text{lab}} \sim 550$ MeV/c in nuclear matter. This is a particular representation of the two-meson cloud contribution to the coupling of the Θ^+ pentaquark in nuclei [3, 4]. Another process that does not depend directly on the suppressed $KN\Theta$ coupling involves the unknown $K^*N\Theta$ coupling constant:

$$K^+ p \rightarrow K^{*+} p , \quad K^{*+} n \rightarrow p , \quad (20)$$

or

$$K^+ n \rightarrow K^{*0} p , \quad K^{*0} p \rightarrow p , \quad (21)$$

with higher thresholds than for Eqs. (18) and (19). Estimates for the $K^+p \rightarrow \pi^+\Theta^+$ reaction cross section suggest conservative values of order 0.1 mb [25, 26] which is of the scale needed to support a similar cross section level for $K^+d \rightarrow \Theta^+p$.

V. SUMMARY AND CONCLUSIONS

There is a wide consensus that the impulse-approximation motivated $t\rho$ optical potential cannot reproduce the density dependence suggested by the K^+ -nuclear cross section data for incident momenta in the range $p_{\text{lab}} \sim 450 - 800$ MeV/c. This was first realized by Siegel *et al.* [27] on the basis of old measurements of total cross sections and later on was reinforced [28, 29] using new transmission measurements data of total cross sections [7]. These investigations incorporated conventional medium effects such as off-shell dependence of the KN t matrix, Fermi averaging and the Pauli exclusion

principle. The revised values of total cross sections, as well as the new reaction cross sections [8] which were subsequently extracted from these same transmission measurements, have led us together with Mareš [5, 6] to look for density dependence mechanisms that could resolve the striking discrepancy between experiment and theory. We have argued recently that the extra reactivity revealed by the K^+ - nucleus cross-section data is simply explained by adding a two-nucleon absorption channel $K^+nN \rightarrow \Theta^+N$ that couples in the $\Theta^+(1540)$ pentaquark in a way which does not involve the apparently suppressed $KN\Theta^+$ coupling [2]. The plausibility of this working hypothesis has been demonstrated very recently in Ref. [4] by evaluating the *unsuppressed* meson-cloud $K\pi N\Theta^+$ coupling which gives rise naturally to this two-nucleon absorption channel, with the same order of magnitude of K^+ absorption cross section as worked out by us [2]. We wish to emphasize that this explanation does not require the assumed $S = +1$ pentaquark degrees of freedom to be materialized as a *narrow* $\Theta^+(1540)$ KN resonance, it only assumes that pentaquark degrees of freedom are spread over this energy range with sufficient spectral strength. If this is not the case, then the problem of excess reactivity in K^+ -nuclear data remains unresolved, as demonstrated very recently by the new calculations of Ref. [30] (see in particular Figs. 9,10, and 12).

In the present work, we have successfully reproduced the available K^+ - nucleus integral (total as well as reaction) cross-section data on the four nuclear targets used in the energy range specified above [7, 8], and also the elastic scattering angular distributions on ${}^6\text{Li}$ and ${}^{12}\text{C}$ at $p_{\text{lab}} = 715$ MeV/c [12, 13], by adding to the $t\rho$ opti-

cal potential a density-dependent term which simulates absorption channels. The analysis of these data is consistent with an upper limit of about 3.5 mb on the K^+ absorption cross section per nucleon, for Θ^+ production on the denser nuclei of ${}^{12}\text{C}$, ${}^{28}\text{Si}$, ${}^{40}\text{Ca}$, and indicates a sub-millibarn cross section for Θ^+ production on deuterium. For a meaningful measurement of this $K^+d \rightarrow \Theta^+p$ two-body production reaction, an experimental accuracy of 0.1 mb in cross section measurements is required. It should provide a competitive production reaction to the $K^+p \rightarrow \pi^+\Theta^+$ two-body production reaction which is being measured at KEK [14]. For nuclear targets other than deuterium, given the magnitude of the K^+ nuclear absorption cross sections as derived in the present work, (K^+, p) experiments could prove useful. This reaction which has a ‘magic momentum’ about $p_{\text{lab}} \sim 600$ MeV/c, where the Θ^+ is produced at rest, is particularly suited to study bound or continuum states in *hyponuclei* [31]. It might prove more useful than the large momentum transfer (K^+, π^+) reaction proposed in this context [32]. In conclusion, precise low-energy K^+d and K^+ - nuclear scattering and reaction data in the range $p_{\text{lab}} \sim 300 - 800$ MeV/c, and particularly about 400 MeV/c, would be extremely useful to decide whether or not $S = +1$ pentaquark degrees of freedom are involved in the dynamics of K^+ - nuclear systems

Acknowledgments

This work was supported in part by the Israel Science Foundation grant 757/05.

-
- [1] G. Trilling in *Reviews of Particle Physics* edited by S. Eidelman *et al.* (Particle Data Group Collaboration), Phys. Lett. B **592**, 1 (2004).
 - [2] A. Gal and E. Friedman, Phys. Rev. Lett. **94**, 072301 (2005).
 - [3] D. Cabrera, Q.B. Li, V.K. Magas, E. Oset, and M.J. Vicente Vacas, Phys. Lett. B **608**, 231 (2005).
 - [4] L. Tolós, D. Cabrera, A. Ramos, and A. Polls, Phys. Lett. B **632**, 219 (2006).
 - [5] E. Friedman, A. Gal, and J. Mareš, Phys. Lett. B **396**, 21 (1997).
 - [6] E. Friedman, A. Gal, and J. Mareš, Nucl. Phys. A **625**, 272 (1997).
 - [7] R. Weiss, J. Aclander, J. Alster, M. Barakat, S. Bart, R.E. Chrien, R.A. Krauss, K. Johnston, I. Mardor, Y. Mardor, S. May Tal-beck, E. Piasetzky, P.H. Pile, R. Sawafta, H. Seyfarth, R.L. Stearns, R.J. Sutter, and A.I. Yavin, Phys. Rev. C **49**, 2569 (1994).
 - [8] E. Friedman, A. Gal, R. Weiss, J. Aclander, J. Alster, I. Mardor, Y. Mardor, S. May-Tal Beck, E. Piasetzky, A.I. Yavin, S. Bart, R.E. Chrien, P.H. Pile, R. Sawafta, R.J. Sutter, M. Barakat, K. Johnston, R.A. Krauss, H. Seyfarth, and R.L. Stearns, Phys. Rev. C **55**, 1304 (1997).
 - [9] R.N. Cahn and G.H. Trilling, Phys. Rev. D **69**, 011501(R) 2004.
 - [10] W.R. Gibbs, Phys. Rev. C **70**, 045208 (2004).
 - [11] A. Sibirtsev, J. Haidenbauer, S. Krewald, and U.-G. Meißner, Phys. Lett. B **599**, 230 (2004); Eur. Phys. J. A **23**, 491 (2005).
 - [12] R.A. Michael, M.B. Barakat, S. Bart, R.E. Chrien, B.C. Clark, D.J. Ernst, S. Hama, K.H. Hicks, W. Hinton, E.V. Hungerford, M.F. Jiang, T. Kishimoto, C.M. Kormanyos, L.J. Kurth, L. Lee, B. Mayes, R.J. Peterson, L. Pinsky, R. Sawafta, R. Sutter, L. Tang, and J.E. Wise, Phys. Lett. B **382**, 29 (1996).
 - [13] R.E. Chrien, R. Sawafta, R.J. Peterson, R.A. Michael, and E.V. Hungerford, Nucl. Phys. A **625**, 251 (1997).
 - [14] Experiment E559 at KEK-PS, K. Imai, Abstract 1WD.00002, 2005, 2nd Meeting of the Nuclear Physics Divisions of the APS and the JPS, Maui, Hawaii, September 2005 (<http://www.aps.org/meet/HAW05>).
 - [15] G. Fricke, C. Bernhardt, K. Heilig, L.A. Schaller, L. Schellenberg, E.B. Shera, and C.W. De Jager, At. Data Nucl. Data Tables **60**, 177 (1995).
 - [16] J.D. Patterson and R.J. Peterson, Nucl. Phys. A **717**, 235 (2003).

- [17] A. Trzcińska, J. Jastrzębski, P. Lubiński, F.J. Hartmann, R. Schmidt, T. von Egidy, and B. Kłos, Phys. Rev. Lett. **87**, 082501 (2001).
- [18] E. Friedman, A. Gal, and J. Mareš, Nucl. Phys. A **761**, 283 (2005).
- [19] R.J. Peterson, Nucl. Phys. A **740**, 119 (2004).
- [20] C.M. Kormanyos, R.J. Peterson, J.R. Shepard, J.E. Wise, S. Bart, R.E. Chrien, L. Lee, B.L. Clausen, J. Piekarewicz, M.B. Barakat, E.V. Hungerford, R.A. Michael, K.H. Hicks, and T. Kishimoto, Phys. Rev. C **51**, 669 (1995).
- [21] M. Ericson and T.E.O. Ericson, Ann. Phys. (NY) **36**, 323 (1966).
- [22] C.J. Batty, E. Friedman, and A. Gal, Phys. Rep. **287**, 385 (1997).
- [23] O. Meirav, E. Friedman, R.R. Johnson, R. Olszewski, and P. Weber, Phys. Rev. C **40**, 843 (1989).
- [24] D. Ashery and J.P. Schiffer, Annu. Rev. Nucl. Part. Sci. **36**, 207 (1986).
- [25] Y. Oh, H. Kim, and S.H. Lee, Phys. Rev. D **69**, 074016 (2004).
- [26] T. Hyodo and A. Hosaka, Phys. Rev. C **72**, 055202 (2005).
- [27] P.B. Siegel, W.B. Kaufmann, and W.R. Gibbs, Phys. Rev. C **31**, 2184 (1985).
- [28] C.M. Chen and D.J. Ernst, Phys. Rev. C **45**, 2019 (1992).
- [29] M.F. Jiang, D.J. Ernst, and C.M. Chen, Phys. Rev. C **51**, 857 (1995).
- [30] H.F. Arellano and H.V. von Geramb, Phys. Rev. C **72**, 025203 (2005).
- [31] A.S. Goldhaber, *Proceedings of the Second LAMPF II Workshop*, edited by H.A. Thiessen, T.S. Bhatia, R.D. Carlini, and N. Hintz, LA-9572-C, Vol. I (1982) 171.
- [32] H. Nagahiro, S. Hirenzaki, E. Oset, and M.J. Vicente Vacas, Phys. Lett. B **620**, 125 (2005).